Temporal and Spatial Variability of Great Lakes Ice Cover, 1973–2010*

JIA WANG

NOAA/Great Lakes Environmental Research Laboratory, Ann Arbor, Michigan

XUEZHI BAI AND HAOGUO HU

Cooperative Institute for Limnology and Ecosystem Research, University of Michigan, Ann Arbor, Michigan

ANNE CLITES, MARIE COLTON, AND BRENT LOFGREN

NOAA/Great Lakes Environmental Research Laboratory, Ann Arbor, Michigan

(Manuscript received 9 September 2010, in final form 11 July 2011)

ABSTRACT

In this study, temporal and spatial variability of ice cover in the Great Lakes are investigated using historical satellite measurements from 1973 to 2010. The seasonal cycle of ice cover was constructed for all the lakes, including Lake St. Clair. A unique feature found in the seasonal cycle is that the standard deviations (i.e., variability) of ice cover are larger than the climatological means for each lake. This indicates that Great Lakes ice cover experiences large variability in response to predominant natural climate forcing and has poor predictability. Spectral analysis shows that lake ice has both quasi-decadal and interannual periodicities of ~8 and ~4 yr. There was a significant downward trend in ice coverage from 1973 to the present for all of the lakes, with Lake Ontario having the largest, and Lakes Erie and St. Clair having the smallest. The translated total loss in lake ice over the entire 38-yr record varies from 37% in Lake St. Clair (least) to 88% in Lake Ontario (most). The total loss for overall Great Lakes ice coverage is 71%, while Lake Superior places second with a 79% loss. An empirical orthogonal function analysis indicates that a major response of ice cover to atmospheric forcing is in phase in all six lakes, accounting for 80.8% of the total variance. The second mode shows an out-of-phase spatial variability between the upper and lower lakes, accounting for 10.7% of the total variance. The regression of the first EOF-mode time series to sea level pressure, surface air temperature, and surface wind shows that lake ice mainly responds to the combined Arctic Oscillation and El Niño–Southern Oscillation patterns.

1. Introduction

The Laurentian Great Lakes, located in the midlatitudes of eastern North America (Fig. 1), contain about 95% of the U.S. and 20% of the world's fresh surface water supply. Nearly one-eighth of the population of the United States and one-third of the population of Canada live within their drainage basin. The ice cover that forms on the Great Lakes each winter affects the regional economy (Niimi 1982), the lake ecosystem (Vanderploeg et al. 1992; Brown et al. 1993; Magnuson et al. 1995), and water level variability (Assel et al. 2004). For example, from the late 1990s to the early 2000s, lake ice cover was much less than normal, which enhanced evaporation and led to a significant water level drop of as much as 3–4 ft (1–1.3 m), depending on which lake (Sellinger et al. 2008). Lower water levels have a significant impact on the Great Lakes economy. Over 200 million tons of cargo are shipped every year through the Great Lakes. Since 1998 when water levels took a severe drop, commercial ships were forced to light-load their vessels. For every inch of clearance that these oceangoing vessels lost because of low water levels, $11,000–$22,000 in profits per day was lost depending on

* Great Lakes Environmental Research Laboratory Contribution Number 1604.

Corresponding author address: Jia Wang, NOAA/Great Lakes Environmental Research Laboratory, 4840 S. State Rd., Ann Arbor, MI 48108-9719.
E-mail: jia.wang@noaa.gov

DOI: 10.1175/2011JCLI4066.1

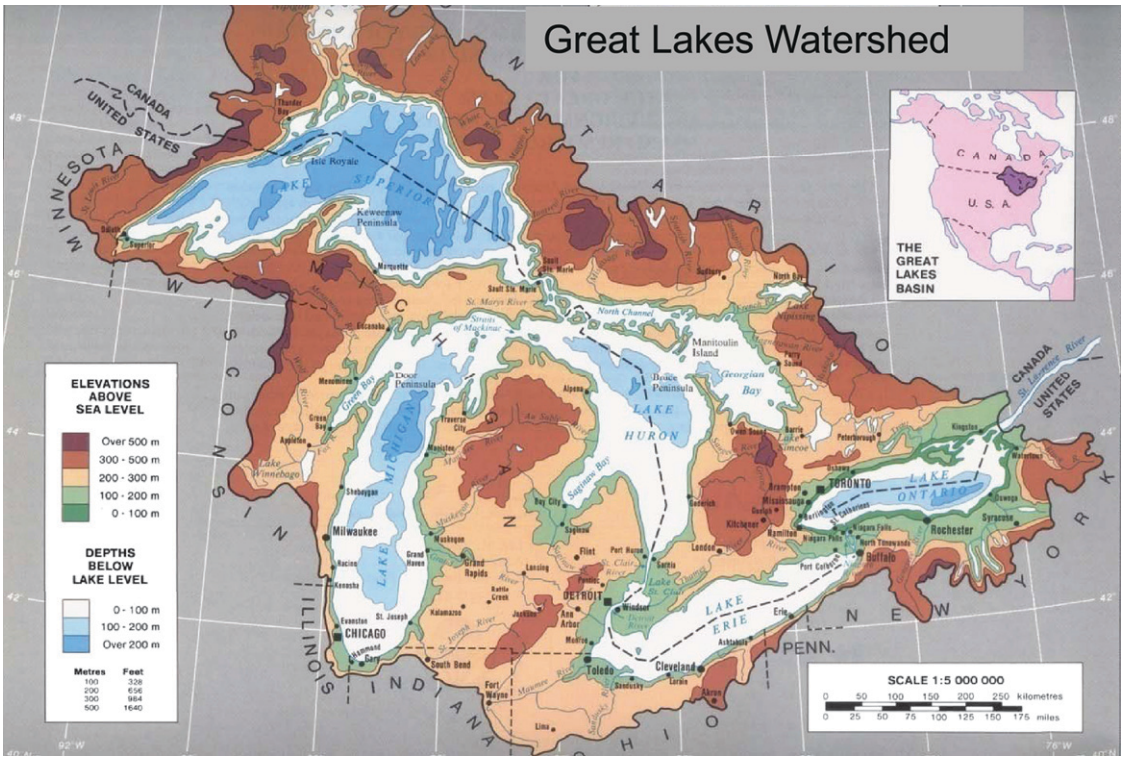

FIG. 1. The Great Lakes watershed and topography. The average lake water depths (surface areas) for Lakes Superior, Michigan, Huron, St. Clair, Erie, and Ontario are 148 (82 400), 84 (58 000), 59 (59 596), 3 (1114), 19 (25 744), and 85 (19 500) m (km^2), respectively.

cargo type. Hydropower plants have also been affected by low water levels; several New York and Michigan plants were run at reduced capacity, forcing them to buy higher priced energy from other sources, and passing on the higher costs to consumers.

Lake ice cover is also a sensitive indicator of regional climate and climate change (Smith 1991; Hanson et al. 1992; Assel and Robertson 1995; Assel et al. 2003; Wang et al. 2010a). Seasonal ice cover repeats each year with large interannual variability. For example, the maximum ice coverage over all of the Great Lakes was 95% in 1979 and only 11% in 2002. Possible contributors include interannual and interdecadal climate variability, and long-term trends, possibly related to global climate warming. Studies of the relationship between interannual variability of ice cover on the Great Lakes and large-scale atmospheric circulation show that teleconnection patterns such as the Pacific–North America (PNA) (Wallace and Gutzler 1981), the Tropical–North Hemisphere (TNH), the North Atlantic Oscillation (NAO) or the Arctic Oscillation (AO) (Thompson and Wallace 1998; Wang and Ikeda 2000, 2001; Wang et al. 2005), the Polar/Eurasian (POL), and the West Pacific (WP), etc., are associated with anomalous ice cover on the Great Lakes (Assel and Rodionov 1998, Assel et al. 2003; Rodionov and Assel 2000, 2001). Combinations of threshold values (both positive and negative) of the POL, PNA, and TNH indices accounted for much of the interannual variation of winter severity, while threshold values of the multivariate El Niño–Southern Oscillation (ENSO) index and the TNH index were found to be useful in modeling Great Lakes annual maximum ice cover variations. A 30-day ice forecast model has been developed using linear regression with teleconnection indices as input (Assel et al. 2004).

Even in response to the same climate forcing, Great Lakes ice may experience different spatial and temporal variability related to each lake's orientation, depth (i.e., water heat storage), and turbidity (i.e., albedo due to sedimentation). To project seasonal and interannual variability of lake ice using statistical analysis, the first step is to investigate the predictability, which is measured by the ratio of the mean (climatology) to standard deviations (i.e., variability). Generally speaking, the larger the ratio, the higher the predictability. In other words, if the standard deviation is larger than the mean, the predictability is poor. Thus, in this study, we try to reveal the spatial and temporal characteristics of ice cover in each lake for a better understanding of Great Lakes ice variability in response to a changing climate. For example,

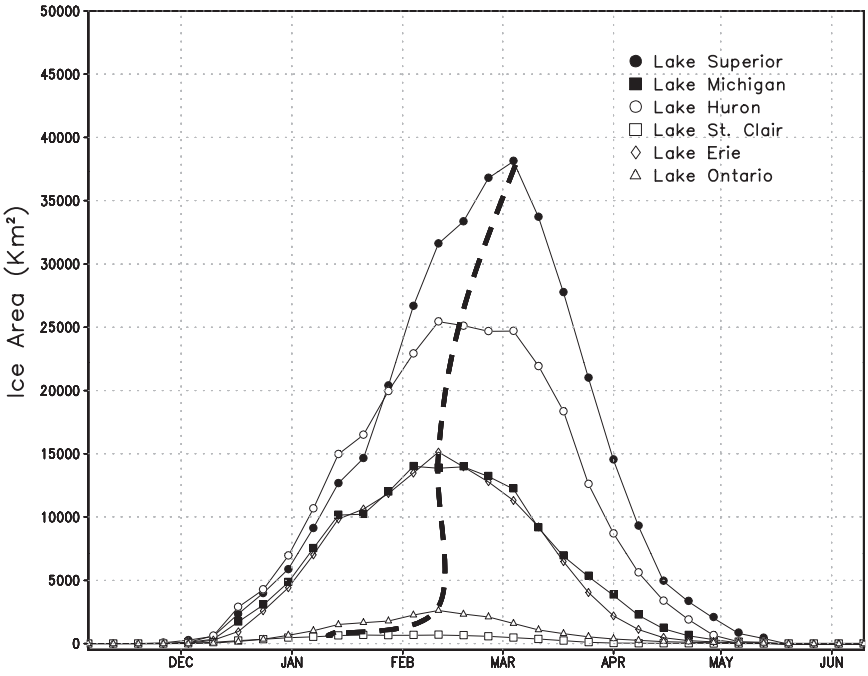

FIG. 2. The NIC twice-weekly average ice cover in the Great Lakes for the period 1973–2010. The vertical dashed line indicates the progression of ice cover maximum in each lake.

under the same climate forcing, lake ice may respond differently in the upper and lower Great Lakes.

2. The data

Systematic lake-scale observations of Great Lakes ice cover began in the 1960s by federal agencies in the United States (U.S. Army Corps of Engineers and U.S. Coast Guard) and Canada (Atmospheric Environment Service, Canadian Coast Guard) to support early and late season navigation, the closing of the navigation season in winter, and the opening of navigation in spring. Observations were made at irregular intervals primarily to support operational activities. Ice charts depicting ice concentration patterns and ice extent were constructed from satellite imagery, side-looking airborne radar imagery, and visual aerial ice reconnaissance (Assel and Rodionov 1998).

Two datasets were used in this study: one from the Canadian Ice Service (CIS) and the other from the NOAA National Ice Center (NIC). The CIS data is from 1973 to 2000. From 1989 to present, these agencies have coordinated their data. During the ice year, each agency has at least one chart per week; more frequently during ice-on (or ice onset) and ice-off (or ice offset) periods to aid navigation. The 1973 ''ice year'' refers to the period from November 1972 to May 1973. Satellite-retrieved ice concentration was derived from NIC Great Lakes Ice Analysis Charts, which are based on *Radarsat-2*, *Envisat*, the Advanced Very High Resolution Radiometer (AVHRR), the Geostationary Operational and Environmental Satellites (GOES), and the Moderate Resolution Imaging Spectroradiometer (MODIS).

The weekly/monthly climatology of the period 1973–2010 was analyzed. The weekly/monthly mean value (i.e., climatology) was subtracted from the individual weeks/months to obtain the weekly/monthly anomalies. Annual-averaged ice cover values were obtained by averaging data in the whole winter season (i.e., ice year). National Centers for Environmental Prediction (NCEP) reanalysis data for the period 1973–2010 were used to investigate the correlation between the major lake ice modes in response to the climate patterns.

3. Results: Regional characteristics, seasonality, and interannual variability

a. Seasonal cycle

The seasonal ice cover cycle (Figs. 2–3) is computed for the six lakes based on the 1973–2010 data (Fig. 4). The typical seasonal ice cycle of the Great Lakes consists of an initial formation (ice onset) period, followed by a growing period in which the annual maximum areal extent is reached, then a melting (break-up) period. The typical ice cycle has an ice-on date on all lakes occurring in late November to early December. Ice forms on Lake

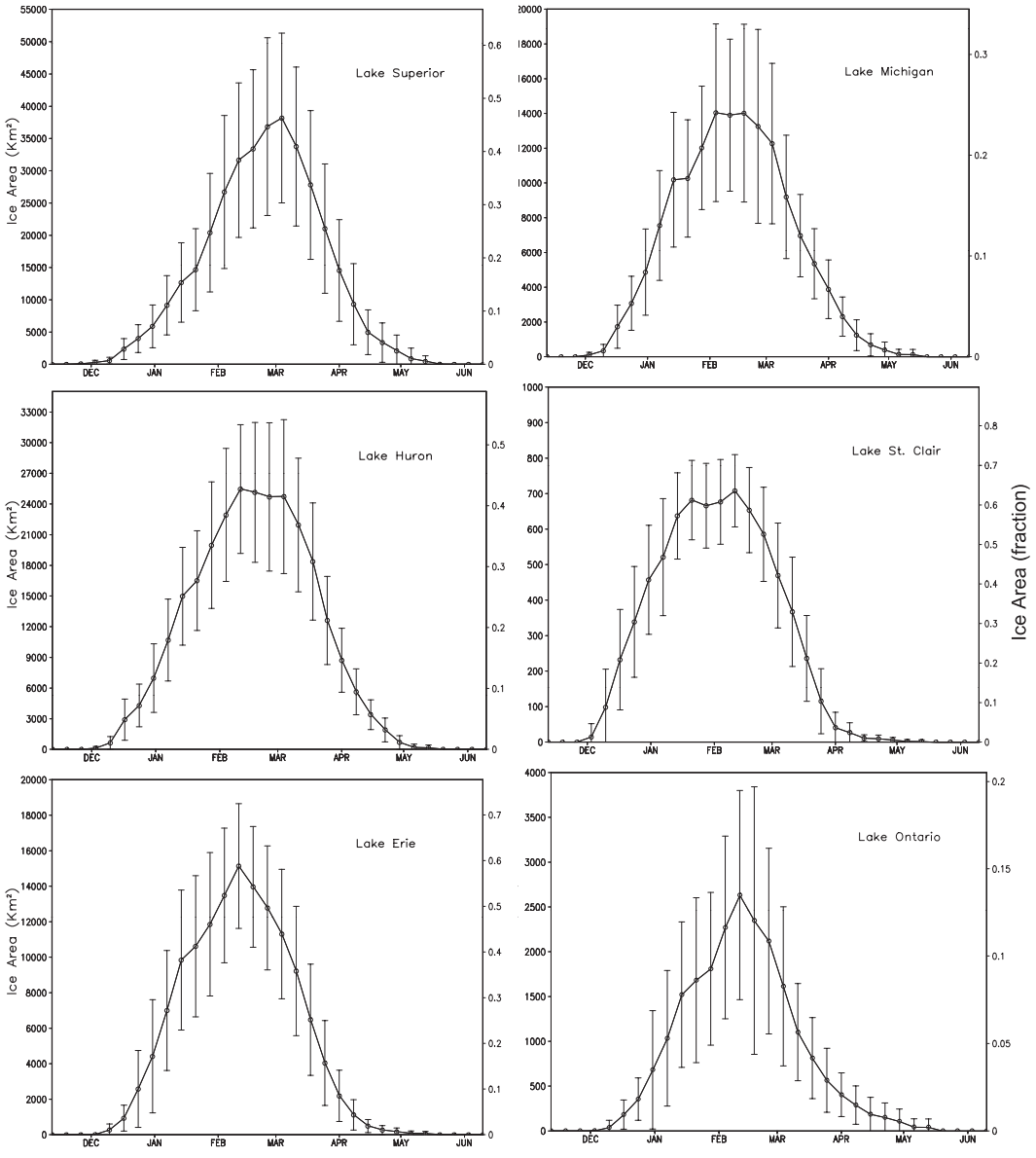

FIG. 3. Variation of weekly ice coverage [lake ice area (km^2), left vertical axes and in fraction divided by the lake surface area, right vertical axes] of the six lakes for the period 1973–2010 with one std dev by the vertical bars.

Superior earlier (week 46) than other lakes. Ice-onset occurs in week 47 on Lakes Michigan, Huron, and St. Clair; and Lakes Erie and Ontario have ice onset in week 48. The growing period of ice cover is about 14–15 weeks. Lake Superior reaches the seasonal maximum extent by week 9 (early March), while other lakes reach maximum ice coverage around week 6. Lake Ontario ice extent has the smallest proportion of its surface area among all the lakes, and has the least statistical significance. The growth of ice cover is remarkably similar in all of the Great Lakes. Figure 2 also shows the progression of maximum ice cover for each lake.

The decrease in ice cover following early March is also quite similar in all lakes. Ice cover on the lower lakes (St. Clair, Erie, and Ontario) breaks up in week 7, earlier than the upper lakes: Superior in week 10, Michigan in week 8, and Huron in week 10. Ice offset occurs in Lake St. Clair in week 18, Erie in week 19, and in other lakes in week 20. Table 1 summarizes these basic statistics.

Based on Fig. 3, it is apparent that there is a local minimum in ice cover for Lake St. Clair in week 4; and there are dual maxima at weeks 3 and 6. This indicates that the large intraseasonal variations may come from

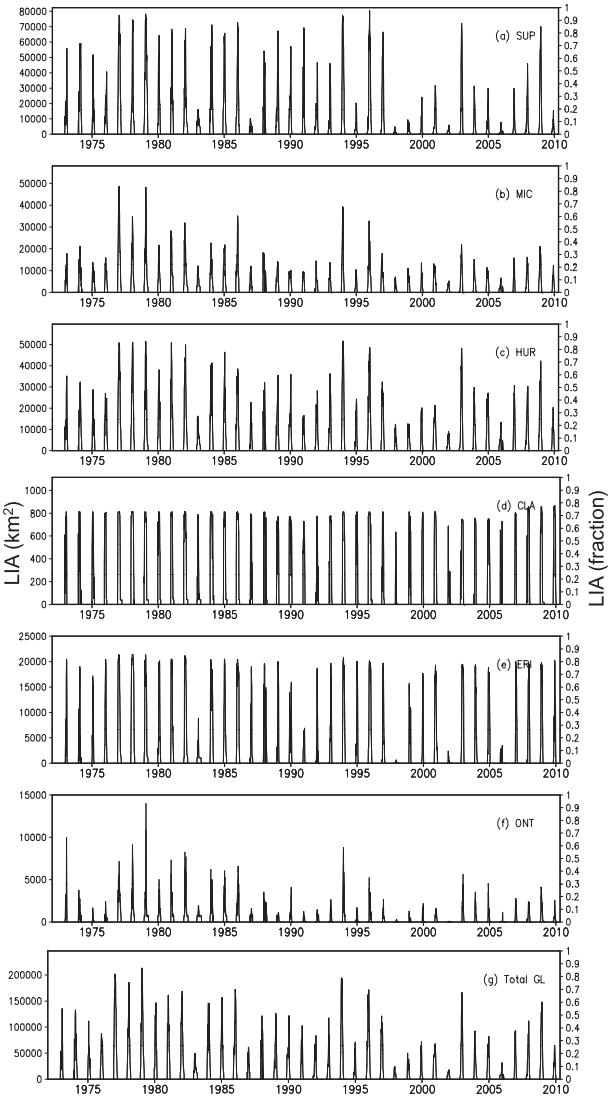

FIG. 4. Weekly time series of LIA for (a)–(f) each of the six lakes and (g) total Great Lakes during the period 1973–2010. Units for lake ice area are km^2 (left vertical axes) and fraction divided by the lake surface area (right vertical axes).

large interannual variability of lake ice in response to extreme weather events that are controlled by the natural internal climate patterns such as AO and ENSO.

b. Variations

The corresponding weekly variations, defined by standard deviations (STDs) of annual ice covers, are also shown in Fig. 3. The months with the largest standard deviations are those most sensitive to atmospheric forcing, and the records with large standard deviations are the periods for better detecting interannual and decadal variability. One unique feature of Great Lakes ice cover, in contrast to Arctic sea ice cover (Wang and Ikeda 2001), is that the STDs are equivalent or even larger in magnitude than the means in the deep-water lakes, while STDs of sea ice are much smaller than the means in the Arctic Ocean (Wang and Ikeda 2001). This indicates that 1) the natural variability of lake ice cover due to natural internal climate forcing is large (Wang et al. 2010a) and 2) the predictability of lake ice cover using both statistical and numerical models is generally poor, particularly for interannual time scales. For example, Lake Ontario has the largest STDs compared to its mean, while Lake St. Clair has the smallest STDs. This implies that ice cover in Lake St. Clair has the best predictability, while ice cover in Lake Ontario has the poorest predictability among all the lakes, although the overall predictability in all lakes is poor.

TABLE 1. Statistics of dates (week) of ice onset, maximum ice coverage, break up, and ice offset in the Great Lakes for the 1973–2010 period.

Week	Superior	Michigan	Huron	St. Clair	Erie	Ontario
Ice onset	46	47	47	47	48	48
Max/peak	9	6	6	6	6	6
Break up	10	8	10	7	7	7
Ice offset	21	20	20	18	19	19

The reason is that the internal variability of natural climate patterns such as ENSO and AO/NAO are poorly predicted (Wang et al. 2010a). Bai et al. (2010, 2012) revealed that both ENSO and AO/NAO have impacts on lake ice; nevertheless, none of them dominates the Great Lakes. However, using both ENSO and AO/NAO indices, lake ice can be projected on the intraseasonal time scale, but has poor predictability on the interannual time scales (from year to year). Thus, short-term numerical prediction based on short-term weather prediction is an alternative to provide relatively accurate prediction of lake ice on synoptic time scales (Wang et al. 2010b).

c. Interannual variability

Time series of weekly ice cover area for all six lakes for the period 1973–2010 have been constructed (Fig. 4), defined as the product of ice concentration and grid area (Wang et al. 1994). All lakes have strong interannual variability of ice cover. However, there are two types of regional features: deep water and shallow water lakes. In the shallow water lakes such as Lakes St. Clair (3 m on average) and Erie (19 m on average), there is almost complete ice cover in winter except in 1992 and 2002 for St. Clair, and 1983, 1991, 1998, 2002, and 2006 for Lake Erie. This indicates that using only lake ice area (LIA) is not sufficient to detect the climate signals in Lakes St. Clair and Erie since the ice area is constrained by the

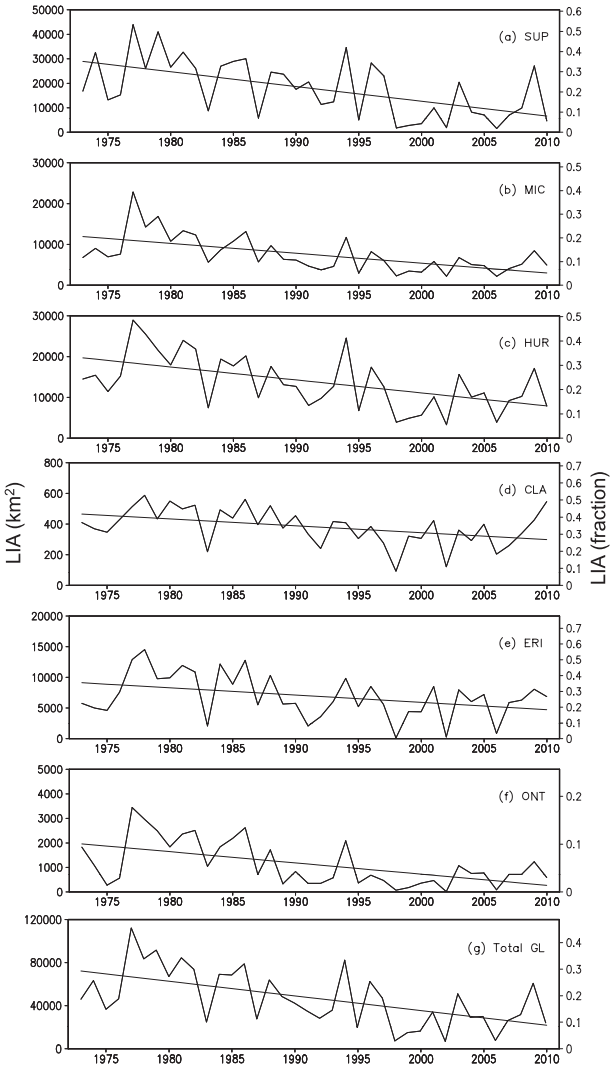

FIG. 5. Annual-mean lake ice area for (a)–(f) each of the six lakes and (g) total Great Lakes ice anomaly during the period 1973–2010. The linear lines are the trend in annual lake ice coverage calculated from the least squares fit method. Unit for the vertical axes is km^2.

bathymetry—the so-called boundary constraint (Wang et al. 1994). Under the boundary constraint, even though the ice area no long increases, ice thickness can still increase in winter. Thus, lake ice thickness must be used to study lake ice in response to a changing climate. However, in the deep-water lakes (Superior: 148 m; Huron: 59 m; and Ontario: 85 m), ice area (extent) can be used to detect climate signals since ice rarely completely covers the lakes. On Lake Erie, the least ice cover was found in 1983, 1991, and 1998, spaced by 7–8 yr, but more frequently since 1998 with a period of about 3–4 yr. This implies that interannual variability of the climate patterns tends to be greater in the Great Lakes in the past decade. In the deep-water lakes, it is possible to detect climate signals using the ice cover area since the boundary constraint is weak.

To investigate interannual variability, the time series of annual-mean lake ice coverage for each lake (Fig. 5) is calculated by averaging over the ice season from the original data (Fig. 4). There is large interannual variability with temporal correspondence among all of the lakes, implying that the major response of lake ice to climate forcing is basically uniform across the Great Lakes watershed since the spatial scale of the Great Lakes is small compared to the teleconnection patterns excited by phenomena such as ENSO and AO/NAO.

We further examined the spectral characteristics of the 38-yr time series of the six lakes (Fig. 6). The main periods are ~8 and 3–5 yr. Lakes Michigan, Huron, St. Clair, and Erie have two periods: 8 and 3.8 yr. The former may be related to AO/NAO, and the latter may be related to ENSO, since both ENSO and AO have impacts on Great Lakes ice cover (Bai et al. 2010, 2012); the AO/NAO has significant decadal to quasi-decadal time scales (7–8 yr) (Wang et al. 1994; Mysak et al. 1996; Wang and Ikeda 2001; Wang et al. 2005), while ENSO basically possesses strong interannual time scales of 3–5 yr.

d. Long-term trend

Ice cover on the Great Lakes has been declining since 1973. Figure 5 and Table 2 show the linear trends for the six lakes. The linear trend was estimated using least squares regression (LSR). The linear equation is in the form: $x = a + bt$, where x is the lake ice area (LIA), t is the year starting from 1973, a is constant (the x-intercept constant: value for $t = 1973$), and b is the slope of the line (the rate of change in x with a time increment of t).

Lake ice annual mean ice cover in all lakes shows a significant negative trend (Fig. 5), indicating that the ice extent in the Great Lakes has been decreasing since the 1970s. The negative trends vary from lake to lake (from -1.3% to -2.3% yr^{-1}, Table 2). Lake Ontario has the largest negative trend (-2.3% yr^{-1}), Lakes Superior and Michigan place second (-2.0% yr^{-1}), and Lakes Erie and St. Clair have the smallest negative trend: -1.3% and -1.0% yr^{-1}, respectively. This translates to a total loss of annual lake ice coverage over the entire 38-yr record from 1973 to 2010 in Table 2 (last row), which varies from 50% in Lake Erie to 88% in Lake Ontario. The total loss for overall Great Lakes ice coverage is 71%, while Lake Superior places second with a 79% loss.

Note that the trends calculated within a specific period of time such as 1973–2010 can only be applicable to the same period and cannot be extrapolated to the future and back to the past. It should not be interpolated to

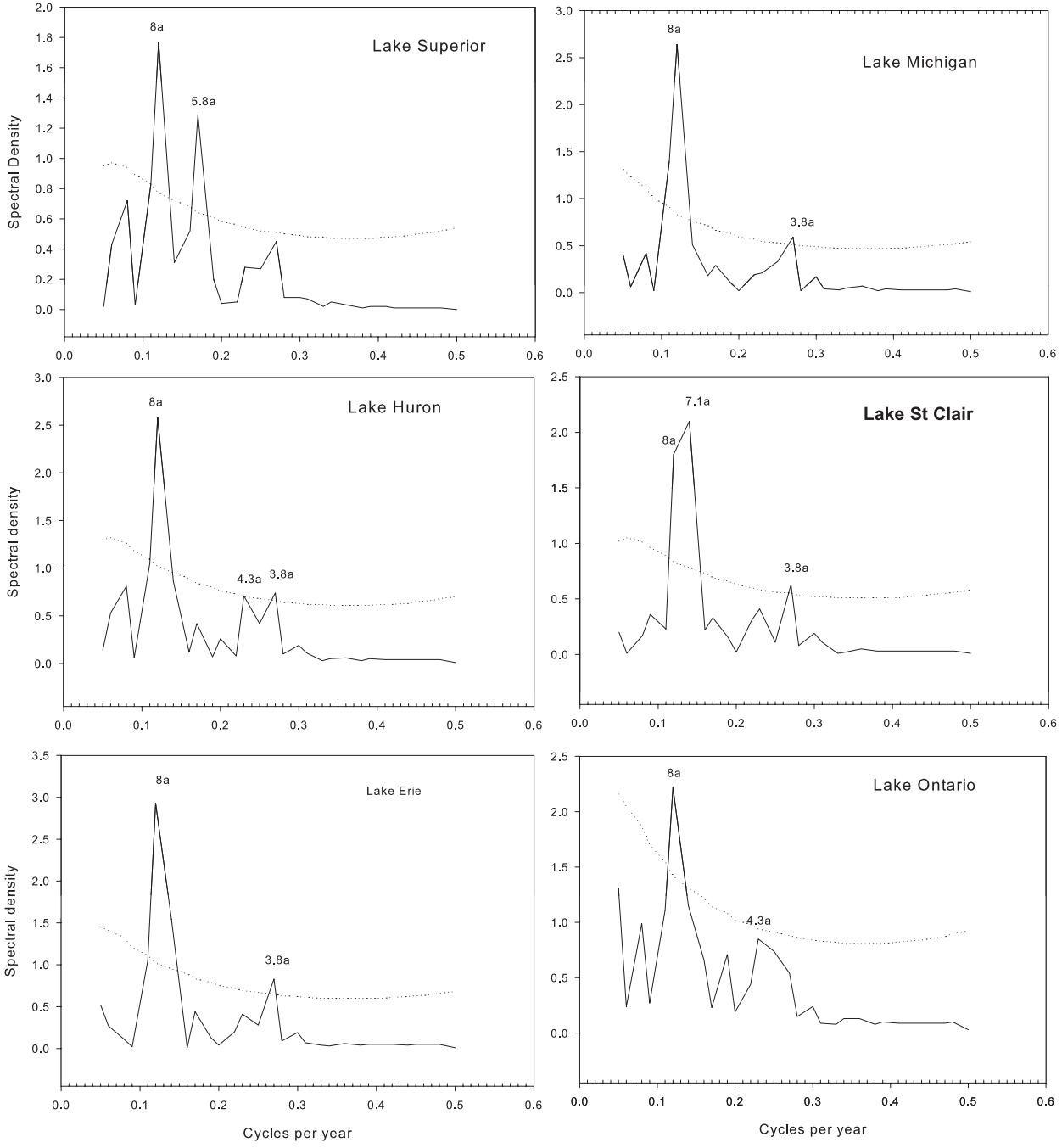

FIG. 6. Spectral analysis of LIA anomalies in all six lakes with the linear trends removed. The dotted curves are the 95% significance level. The peaks are marked with the corresponding periods in years.

a period shorter than the time series of the data from which the trends are derived since there are decadal and multidecadal changes in lake ice cover.

To search for factors responsible for the lake ice trend, the winter surface air temperature (SAT) trend over the Northern Hemisphere was calculated for the period 1973–2010 (Fig. 7). The SAT trend over the Great Lakes ranges from ~0.4°C decade^{-1} over the lower lakes to ~0.6°–0.7°C decade^{-1} over the upper lakes, with Lake Superior being the highest (0.7°C decade^{-1}). This is consistent with the upward trend of Lake Superior water temperature (Austin and Colman 2007). They found that summer (July–September) surface water temperatures have increased approximately 2.5°C over the interval 1979–2006,

TABLE 2. Trends in annual lake ice coverage calculated by linear least squares fit for the period 1973–2010 (see text for detail): a is the intercept constant (the value in year 1973, km^2); b the slope of the line (the rate of change in ice area with time, km^2 yr^{-1}); (b/a) × 100% is the relative trend in annual lake ice coverage (% yr^{-1}); and total loss (%) is the total reduction of the annual lake ice area over the entire 38-yr record (from 1973 to 2010).

	Superior	Michigan	Huron	St. Clair	Erie	Ontario	Total GL
a	28 938.148	11 932.121	19 711.088	466.027	9136.481	19 60.767	72 164.531
b	−599.032	−241.424	−323.244	−4.482	−119.046	−45.642	−1343.403
$b/a \times 100\%$	−2.070	−2.023	−1.640	−0.962	−1.303	−2.328	−1.862
Total loss (%)	−79	−77	−62	−37	−50	−88	−71

significantly in excess of regional atmospheric warming. This excessive warming of lake water temperature relative to the local surface air temperature is caused by a positive ice/water albedo feedback (Wang et al. 2005) due to the declining winter ice cover (Austin and Colman 2007).

4. Spatial and temporal patterns of lake ice cover

To reveal the prevailing spatial patterns of lake ice cover variability, an EOF analysis of LIA anomalies of six lakes (for spatial pattern) for the period 1973–2010 (for temporal variability) was conducted with the lake ice trend removed, following the same approach of Wang and Ikeda (2001). The leading lake ice mode (Fig. 8) accounts for 80.8% of the total variance. Lake ice anomalies in the six lakes fluctuate in phase (i.e., same sign) in response to climate forcing (Fig. 8a). Note that the amplitude (Fig. 8a) of the shallow-water lakes such as Huron (0.81) and Erie (0.88) [except for Lake St. Clair (0.74), because of the boundary constraint of ice cover growth in response to climate forcing] are larger than the deep-water lakes such as Superior (0.69), Michigan (0.73), and Ontario (0.76). This implies that the shallow-water lakes are more sensitive to a climate forcing because of their shorter memory of water heat capacity than the deep-water lakes. The deep-water lakes, in particular Lake Superior, have large water heat capacity and inertia, which can modulate ice-on, ice-off, and ice duration dates under the same atmospheric forcing. The mechanism behind this can be explained by the positive ice–water albedo feedback (Austin and Colman 2007; Wang et al. 2005) since an increase in lake surface temperature (i.e., heat capacity) due to solar radiation in deep-water lakes can be amplified by the positive ice–water albedo feedback, compared to in the shallow-water lakes. The time series obviously shows a mixed long-term trend and decadal and interannual variability. The major periods of the first time coefficient are 8 and 4 yr (Fig. 8b).

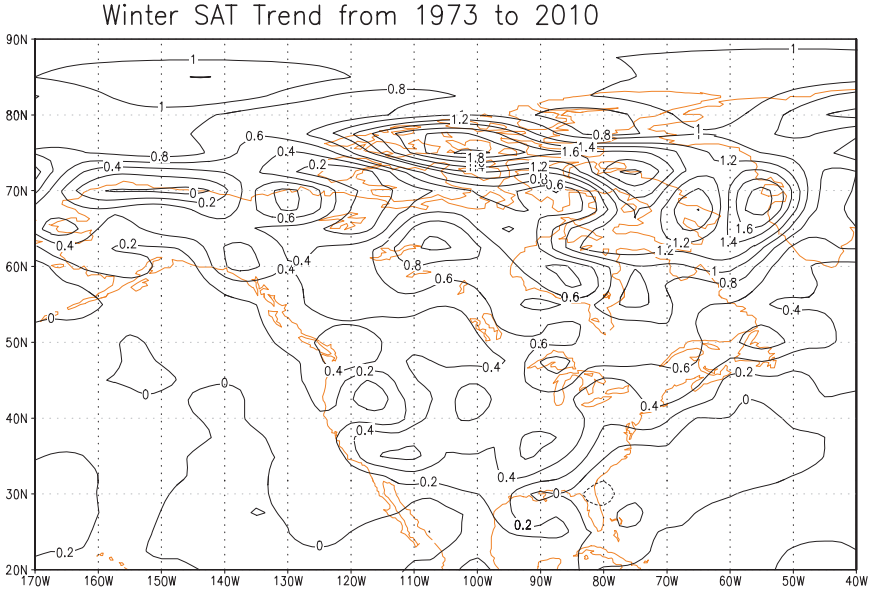

FIG. 7. Winter SAT trend (°C decade^{-1}) for the period 1973–2010, calculated using a least squares fit.

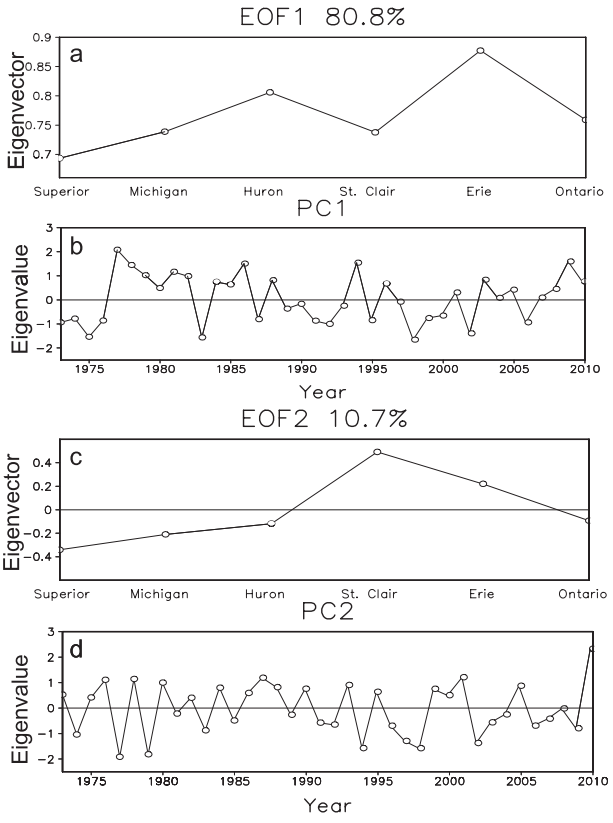

FIG. 8. The first two leading EOF modes of the eigenvectors (spatial pattern) and the time series of the eigenvalues or the coefficients (temporal pattern) of LIA anomalies for the period 1973–2010 (with the linear trends removed): (a),(c) eigenvectors and (b),(d) eigenvalues.

The second mode accounts for only 10.7% of the total variance. It captures a seesaw pattern (out of phase or opposite sign) between the upper lakes (Superior and Michigan) and the lower lakes (St. Clair and Erie), with Lakes Huron and Ontario being in the middle (near the zero line) (Fig. 8c). It was expected that Lake Ontario ice would have similar features as the lower lakes; nevertheless, the variation of Lake Ontario ice is similar to Lake Huron. Lake Ontario has the smallest amount of ice cover relative to its surface area (Fig. 2) and has the smallest seasonal (Figs. 2–4) and interannual (Fig. 5) variability. Since 1990 the year-to-year change in Lake Ontario was smaller than any of the other lakes. Thus, the climate signal derived from ice cover is insignificant. This unexpected variability needs further in-depth investigation. In the deep-water lakes, heat storage in the water column plays a more important role than in the shallow-water lakes and needs to be investigated in depth.

To quantitatively understand the two LIA patterns in the context of atmospheric circulation anomalies, the time series of the first EOF mode are regressed to the Northern Hemisphere sea level pressure (SLP) (Fig. 9a),

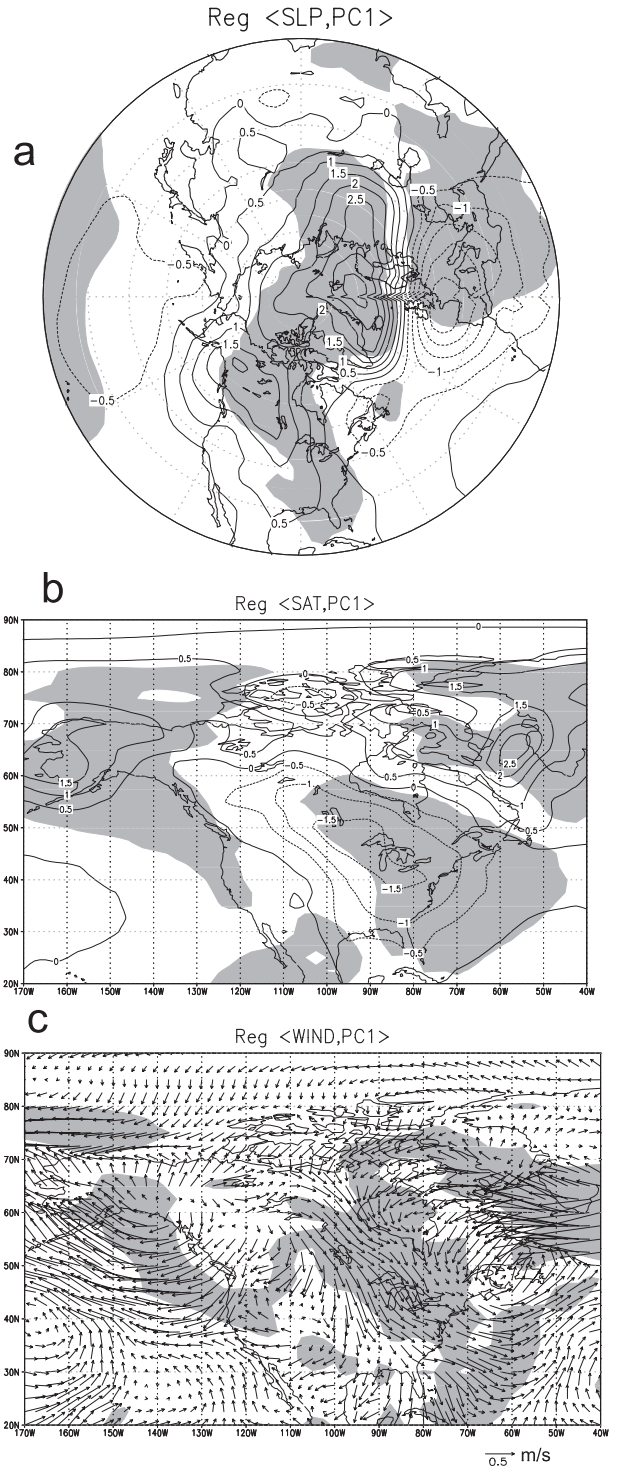

FIG. 9. The anomalous (a) SLP (hPa), (b) SAT (°C), and (c) surface wind (m s^{-1}) maps regressed to the time series of the first EOF mode of lake ice for the period 1973–2010. The shaded areas are over 95% significance level. Contour intervals for (a) SLP and (b) SAT are 0.5 hPa and 0.5°C. The unit of anomalous winds in (c) is in 0.5 m s^{-1}, as shown by the vector at the bottom.

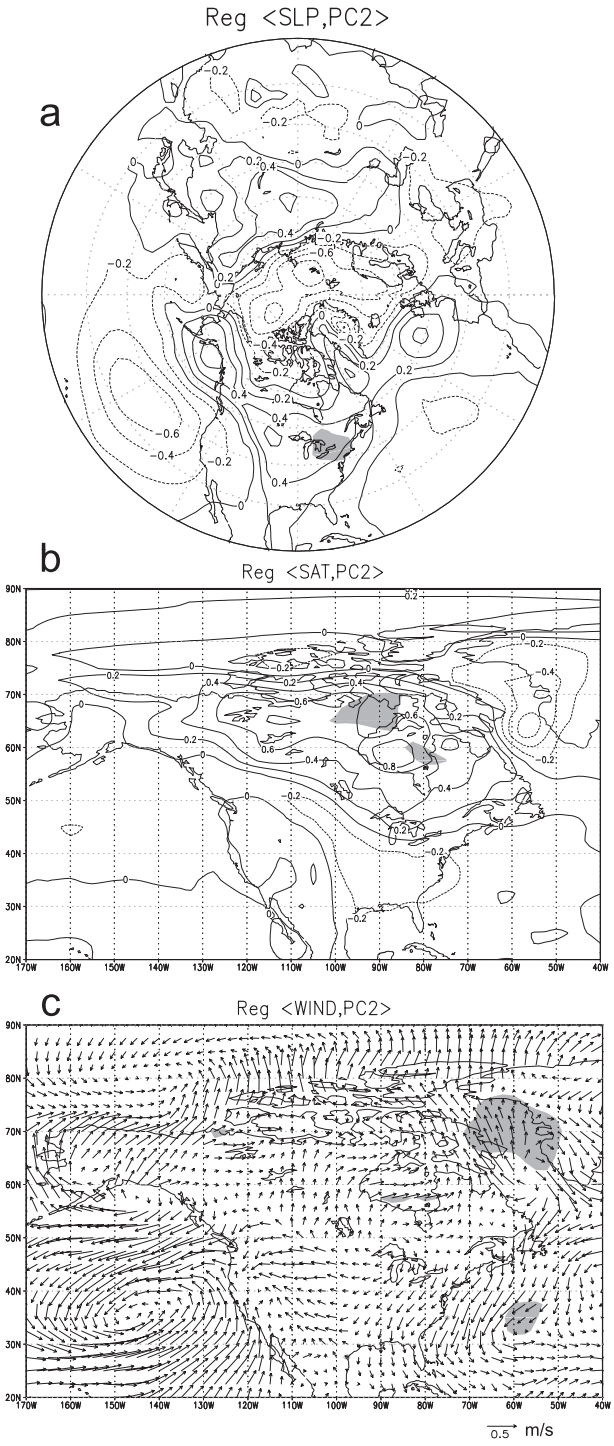

FIG. 10. As in Fig. 9, but for the second EOF mode of lake ice.

surface air temperature (SAT) (Fig. 9b), and surface wind (Fig. 9c) fields. A remarkable signature is the combination of a negative phase of the AO and La Niña or a negative phase of the PNA (Fig. 9a), which has a positive SLP anomaly in the Arctic and negative SLP anomalies in the subpolar regions, Icelandic and Aleutian lows. The negative center over the central North Pacific is characteristic of the PNA, and the positive center to the northeast is a hybrid of the PNA's northwestern North American center and the AO's Aleutian center. Also, the PNA's southeastern North American center is not evident.

The impact of an AO on the SAT field (Fig. 9b) shows a seesaw pattern in the SAT between the Arctic and northern Europe (−SAT) and Greenland and Labrador Seas (+SAT) (Wang et al. 1994; Mysak et al. 1996; Wang and Ikeda 2000). The impact of the combined −AO and −PNA (La Niña) on SAT over the Great Lakes shows a large −SAT anomaly, consistent with the generalized composite analyses (Bai et al. 2010, 2012). The surface wind anomaly field (Fig. 9c) associated with the SLP anomaly field (Fig. 9a) indicates that strong northwesterly wind anomalies advect cold, dry Arctic air to the Great Lakes region (Fig. 9b). An opposite scenario occurs during the positive phase of the AO and PNA.

Similarly, the time series of the second EOF mode are regressed to the Northern Hemisphere SLP, SAT, and wind fields (Fig. 10). The SLP regression map shows a complicated pattern, similar to the east Pacific pattern, with a significant area covering the Great Lakes (Fig. 9a). The regression map of an anomalous SAT field indicates a north–south gradient with the zero line along a line between Lakes Huron and Ontario, consistent with the second EOF mode (seesaw) of LIA (Fig. 8c). The positive SAT anomaly covers much of Canada with the significance area being over Hudson Bay. The negative SAT anomaly covers much of the Midwest and the East Coast, but not over the 95% significance level (Fig. 10b). The dynamic mechanism can be explained by the (cold) northeasterly wind anomaly in the lower lakes (Fig. 10c), which originates from the Labrador Sea, while over the upper lakes region, the wind anomaly is very small and not statistically significant.

5. Conclusions and discussion

On the basis of the above investigation, the following conclusions can be drawn.

1) The seasonal cycle of lake ice cover for all six lakes experiences similar seasonal variations with some timing difference (lag) from lake to lake. There is a distinct difference between the deep-water and shallow-water lakes in terms of ice-onset and ice-offset timing. For the shallow lakes, ice forms and reaches the maximum earlier than the deep-water lakes, given the same atmospheric conditions.

2) A major finding is that the weekly/monthly standard deviations of lake ice area are equivalent or sometimes even larger than their climatological means, indicating poor predictability of medium- and long-range ice conditions due to large, natural interannual variability.
3) There is a strong natural interannual variability for all the lakes. Spectral analysis shows two significant periods: ~8 and ~4 yr. The former may be related to the AO/NAO, while the latter may be related to ENSO.
4) There is a significant downward trend in lake ice cover for all of the lakes for the period 1973–2010. The largest trend occurs in Lakes Ontario, Superior, and Michigan, while the smallest trend occurs in Lakes St. Clair and Erie (Table 2). This translates into a total loss in all Great Lakes ice coverage of 71% over the entire 38-yr record.
5) EOF analysis shows that the predominant response of lake ice to the atmosphere is in phase for all six lakes, accounting for ~81% of the total variance. However, the second mode (~11%) shows the out-of-phase response between the shallow-water lakes (lower lakes) and the deep-water lakes (upper lakes).
6) The regression analysis shows that the first EOF mode of lake ice mainly responds to the combined AO/NAO and ENSO, along with a long-term trend. The −AO results in a strong northwesterly wind anomaly, advecting cold, dry Arctic air into the Great Lakes region and thus producing a strong negative SAT anomaly over the Great Lakes region and promoting heat loss from the lakes through three mechanisms—longwave radiation, sensible heat flux, and latent heat flux associated with evaporation; vice versa during the +AO/El Niño phase. The second EOF mode of lake ice anomaly basically responds to the similar ''East Pacific'' pattern, resulting in a north–south SAT gradient, consistent with the seesaw pattern of lake ice derived from the EOF analysis of the LIA field (Fig. 8c).

The response of Lake Ontario ice cover is similar to Lake Huron ice cover, which was unexpected. It was thought that Lake Ontario ice variation would be in phase with the lower lakes. There may be several possible explanations. One is that the ice on deep-water lakes has different features from lake ice on the shallow-water lakes since the water heat storage is larger in the former than the latter; thus, the preceding water temperature has significant control of lake ice as SAT. The second reason may be that the zero line of the SAT anomaly lies across Lake Ontario (Fig. 10b), but Lakes Erie and St. Clair are farther into the negative zone. The third reason may be that Lake Ontario has the smallest percentage of ice cover and the least seasonal and year-to-year variations, compared to its lake surface, on all the Great Lakes; thus Lake Ontario's ice signals are weakest of all the lakes.

Acknowledgments. NCEP reanalysis data was provided by the NOAA/OAR/ESRL PSD, Boulder, Colorado, from their Web site at http://www.cdc.noaa.gov/. This study was supported by grants from National Research Council Research Association Fellowship and NOAA GLERL. Support from U.S. EPA's Great Lakes Restoration Initiative (GLRI) to climate change and modeling studies is appreciated. We appreciate Cathy Darnell for her editorial assistance. We particularly thank Dr. John Lenters of University of Nebraska—Lincoln for his valuable comments on the first draft of this paper. We also sincerely thank two anonymous reviewers for their constructive comments, which helped to improve the presentation of the paper.

REFERENCES

Assel, R. A., and D. M. Robertson, 1995: Changes in winter air temperatures near Lake Michigan during 1851–1993, as determined from regional lake-ice records. *Limnol. Oceanogr.,* **40,** 165–176.

——, and S. Rodionov, 1998: Atmospheric teleconnections for annual maximal ice cover on the Laurentian Great Lakes. *Int. J. Climatol.,* **18,** 425–442.

——, K. Cronk, and D. C. Norton, 2003: Recent trends in Laurentian Great Lakes ice cover. *Climatic Change,* **57,** 185–204.

——, S. Drobrot, and T. E. Croley, 2004: Improving 30-day Great Lakes ice cover outlooks. *J. Hydrometeor.,* **5,** 713–717.

Austin, J. A., and S. Colman, 2007: Lake Superior summer water temperatures are increasing more rapidly than regional air temperatures: A positive ice-albedo feedback. *Geophys. Res. Lett.,* **34,** L06604, doi:10.1029/2006GL029021.

Bai, X., J. Wang, C. Sellinger, A. Clites, and R. Assel, 2010: The impacts of ENSO and AO on the interannual variability of Great Lakes ice cover. NOAA Tech. Memo. GLERL-152, 48 pp.

——, ——, ——, ——, and ——, 2012: Interannual variability of Great Lakes ice cover and its relationship to NAO and ENSO. *J. Geophys. Res.,* doi:10.1029/2010JC006932.

Brown, R., W. Taylor, and R. A. Assel, 1993: Factors affecting the recruitment of lake whitefish in two areas of northern Lake Michigan. *J. Great Lakes Res.,* **19,** 418–428.

Hanson, P. H., C. S. Hanson, and B. H. Yoo, 1992: Recent Great Lakes ice trends. *Bull. Amer. Meteor. Soc.,* **73,** 577–584.

Magnuson, J., and Coauthors, 1995: Region 1—Laurentian Great Lakes and Precambrian Shield. *Proc. Symp. Report: Regional Assessment of Freshwater Ecosystems and Climate Change in North America,* Leesburg, VA, U.S. Environmental Protection Agency and U.S. Geological Survey, 3–4. [Available online at http://www.aslo.org/meetings/Freshwater_Ecosystems_Symposium.pdf.]

Mysak, L. A., R. G. Ingram, J. Wang, and A. van der Baaren, 1996: Anomalous sea-ice extent in Hudson Bay, Baffin Bay and the Labrador Sea during three simultaneous ENSO and NAO episodes. *Atmos.–Ocean,* **34,** 313–343.

Niimi, A. J., 1982: Economic and environmental issues of the proposed extension of the winter navigation season and improvements on the Great Lakes-St. Lawrence Seaway system. *J. Great Lakes Res.,* **8,** 532–549.

Rodionov, S., and R. A. Assel, 2000: Atmospheric teleconnection patterns and severity of winters in the Laurentian Great Lakes basin. *Atmos.–Ocean,* **38,** 601–635.

——, and ——, 2001: A new look at the Pacific/North American Index. *Geophys. Res. Lett.,* **28,** 1519–1522.

Sellinger, C. E., C. A. Stow, E. C. Lamon, and S. S. Qian, 2008: Recent water level declines in the Lake Michigan-Huron system. *Environ. Sci. Technol.,* **42,** 367–373.

Smith, J. B., 1991: The potential impacts of climate change on the Great Lakes. *Bull. Amer. Meteor. Soc.,* **72,** 21–28.

Thompson, D. W. J., and J. M. Wallace, 1998: The Arctic Oscillation signature in the wintertime geopotential height and temperature fields. *Geophys. Res. Lett.,* **25,** 1297–1300.

Vanderploeg, H. A., S. J. Bolsenga, G. L. Fahnenstiel, J. R. Liebig, and W. S. Gardner, 1992: Plankton ecology in an ice-covered bay of Lake Michigan: Utilization of a winter phytoplankton bloom by reproducing copepods. *Hydrobiologia,* **243–244,** 175–183.

Wallace, J. M., and D. Gutzler, 1981: Teleconnection in the geopotential height field during the Northern Hemisphere winter. *Mon. Wea. Rev.,* **109,** 784–812.

Wang, J., and M. Ikeda, 2000: Arctic Oscillation and Arctic Sea-Ice Oscillation. *Geophys. Res. Lett.,* **27,** 1287–1290.

——, and ——, 2001: Arctic Sea-Ice Oscillation: Regional and seasonal perspectives. *Ann. Glaciol.,* **33,** 481–492.

——, L. A. Mysak, and R. G. Ingram, 1994: Interannual variability of sea-ice cover in Hudson Bay, Baffin Bay and the Labrador Sea. *Atmos.–Ocean,* **32,** 421–447.

——, M. Ikeda, S. Zhang, and R. Gerdes, 2005: Linking the Northern Hemisphere sea ice reduction trend and the quasi-decadal Arctic Sea Ice Oscillation. *Climate Dyn.,* **24,** 115–130, doi:10.1007/s00382-004-0454-5.

——, X. Bai, G. Leshkevich, M. Colton, A. Clites, and B. Lofgren, 2010a: Severe ice cover on Great Lakes during winter 2008–2009. *Eos, Trans. Amer. Geophys. Union,* **91** (5), 41–42.

——, H. Hu, D. Schwab, G. Leshkevich, D. Beletsky, N. Hawley, and A. Clites, 2010b: Development of the Great Lakes Ice-circulation Model (GLIM): Application to Lake Erie in 2003-2004. *J. Great Lakes Res.,* **36,** 425–436.